

Antarctic ozone depletion and trends in tropopause Rossby wave breaking

T. Ndarana,^{1,2} D. W. Waugh,^{1*} L. M. Polvani,^{3,4} G. J. P. Correa⁵ and E. P. Gerber⁶

¹Department of Earth and Planetary Sciences, Johns Hopkins University, Baltimore, MD, USA

²South African Weather Service, Pretoria, South Africa

³Department of Applied Physics and Applied Mathematics, Columbia University, New York, NY, USA

⁴Department of Earth and Environmental Sciences, Columbia University, New York, NY, USA

⁵Lamont Doherty Earth Observatory, Columbia University, Palisades, NY, USA

⁶Courant Institute of Mathematical Sciences, New York University, New York, NY, USA

*Correspondence to:

D. W. Waugh, Department of Earth and Planetary Sciences, Johns Hopkins University, 320 Olin Building, 3400 North Charles Street, Baltimore, MD 21218, USA.

E-mail: waugh@jhu.edu

Abstract

Trends in summer tropopause Rossby wave breaking (RWB) are examined using meteorological reanalyses and model integrations. The reanalyses for the last 30 years show large increases in RWB on the equatorward side of the tropospheric jet and weak decreases on the poleward side. Comparable changes in RWB are found in general circulation model integrations whose stratospheric ozone differs between 1960 and 2000 levels, but not in integrations that differ only in their greenhouse gas concentrations and sea-surface temperatures. These results indicate that the formation of the ozone hole has led to changes in RWB frequency during southern summer. Copyright © 2012 Royal Meteorological Society

Keywords: ozone hole; Rossby waves; trends

Received: 11 January 2012

Revised: 2 April 2012

Accepted: 2 April 2012

1. Introduction

There have been numerous changes in Southern Hemisphere (SH) tropospheric climate during Austral summer over the last 30 years, including an increase in zonal-mean sea-level pressure difference between the mid- and high latitudes, a poleward shift in the tropospheric westerly jet, and a poleward expansion of the Hadley cell and subtropical dry zone (e.g. Thompson and Solomon, 2002; Hu and Fu, 2007; Previdi and Liepert, 2007). Furthermore, modeling studies indicate that stratospheric ozone depletion is the primary cause for the changes during southern spring and summer (e.g. Son *et al.*, 2009; McLandress *et al.*, 2011; Polvani *et al.*, 2011). Given these changes in the large-scale tropospheric circulation one might expect trends in synoptic-scale systems.

Here we examine changes in SH upper tropospheric Rossby wave breaking (RWB) events (McIntyre and Palmer, 1983) during Austral summer. Changes in these events are of interest as they are linked to weather systems (e.g. cut-off lows (COLs), blocking highs), extreme weather events (e.g. heavy rainfall and floods), and stratosphere–troposphere exchange of trace gases (e.g. Pelly and Hoskins, 2003; Sprenger *et al.*, 2007; Ndarana and Waugh, 2010). The climatological structure and occurrence of near-tropopause RWB in the SH have recently been examined by Ndarana and Waugh (2011) and Wang and Magnusdottir (2011). Wang and Magnusdottir (2011) also examined interannual variations and showed an increasing trend in anticyclonic RWB between 30 and 60°S that

closely matched the trend in the Southern Annular Mode.

In this paper, we reexamine the observed trends in RWB using National Centers for Environmental Prediction/National Center for Atmospheric Research (NCEP/NCAR) reanalyses (Kalnay *et al.*, 1996). We further examine the occurrence and cause of trends in RWB in ‘time-slice’ atmospheric general circulation model integrations that differ in the specified ozone and greenhouse gas (GHG) concentrations and sea-surface temperatures (SSTs). These integrations enable the relative role of ozone depletion and increases in GHGs/SSTs in causing trends in RWB to be evaluated.

2. Data and methods

We study the trends in SH RWB events during December–February (DJF) between 1979 and 2009 using the climatology of these events constructed from NCEP/NCAR reanalyses by Ndarana and Waugh (2011) (NW11, hereafter). The RWB events of interest here occur around the tropopause, and are identified by the overturning of $PV = -1.5$ to -2.5 PVU (where $1 \text{ PVU} = 10^{-6} \text{ m}^2 \text{ s}^{-1} \text{ K kg}^{-1}$) contours on isentropes between 310 and 350 K (see NW11 for details). RWB events are separated into anticyclonic and cyclonic wave breaking events (AWB and CWB, respectively), using the meridional component of the wave activity flux (AWB events have larger positive fluxes, whereas CWB have larger negative fluxes; see NW11). We group all RWB events together within

a given latitude range, regardless of which isentrope they occur on, and examine variations with latitude. If RWB events are identified on multiple isentropes only a single event is retained.

The occurrence of RWB events is also examined in four ‘time-slice’ integrations of the Community Atmosphere Model 3 (CAM3; Collins *et al.*, 2006) described by Polvani *et al.* (2011). The first (‘REF1960’) is a reference simulation in which the SSTs and concentrations of GHGs and ozone are specified using representative values of the year 1960. In the other integrations at least one of these fields was changed to year 2000 values: In the ‘OZONE 2000’ integration the ozone fields were specified at 2000 levels while the other forcing components are kept at 1960 levels; in ‘GHG 2000’ all the forcing fields except ozone were specified at 2000 levels; in ‘BOTH 2000’ all forcings are specified at 2000 levels. In all integrations the SSTs and sea-ice concentrations are obtained from the Hadley Center dataset (Rayner *et al.* 2003), GHG concentrations are from the Special Report on Emissions Scenarios (SRES) A1B scenario (Nakicenovic and Swart, 2000), and the ozone fields are those used for the CMIP5 Model Intercomparison Project (Cionni *et al.*, 2011). The algorithms used to identify RWB in the NCEP/NCAR reanalyses are applied to 10 years of DJF daily output from the end of 60 year integrations.

3. NCEP/NCAR reanalyses

A recent study by Wang and Magnusdottir (2011) has shown trends in SH RWB on the 350 K isentropic surface in austral summer (DJF) over the past 30 years. We reexamine this issue here using a different algorithm to identify RWB events and, more importantly, focus on RWB that occurs on the tropopause. Wang and Magnusdottir (2011) examined RWB on the 350 K for a wide range of PV values that captured RWB from low to high latitudes. However, at middle and high latitudes the 350 K surface is much higher than the tropopause, and there may not be a one-to-one correspondence between RWB at 350 K and on the tropopause.

We first revisit the climatological variation of RWB occurrence with latitude. As shown in the black curve in Figure 1(c), there is local minimum in the frequency of RWBs around 50°S, which is the mean location of the jet core (see black contours in Figure 1(a)). Local maxima occur at 30 and 65°S, which are regions of large meridional velocity gradients. (The rapid decrease in RWB frequency north of 20°S and south of 75°S is related to the range of isentropes examined, i.e. the 310–350 K isentropics cross the tropopause between 20 and 75°S.) On the equatorward side of the jet there is anticyclonic shear, and the RWB in this region is almost exclusively anticyclonic, see red curve in Figure 1(c) which shows the frequency of AWB (see also NW11 and Wang and Magnusdottir

(2011)). Conversely, on the poleward side of the jet the shear is cyclonic and the majority of the RWB is cyclonic (see blue curve in Figure 1(c)).

Large changes in the SH tropospheric circulation in DJF have been observed over the last three decades (Section 1). In particular, there has been a weakening of the zonal wind on the equator side of the jet (40°S) and a strengthening on the polar side (60°S), see Figure 1(a). These changes correspond to a poleward shift of the tropospheric jet, and the jet at 300 hPa has moved south around 4°, see Figure 1(b). A similar shift is observed if winds at 850 hPa are used to diagnose the jet latitude.

To explore long-term changes in RWB that accompany the shift in the jet we examine the temporal variations in the number of RWB events per DJF. We consider first the RWB on the equatorward side of the jet, where the zonal flow has decelerated as the jet has moved poleward. The red curve in Figure 1(d) shows the temporal variation for RWB events within 30–40°S. There are considerable year-to-year variations in the number of RWB events, but there is a clear positive trend. The number of RWB events per season has increased by around 70% over the 30 year period (this trend is significant at the 99% confidence level). Similar, positive trends in RWB are observed for all latitudes between 25 and 50°S, see Figure 1(e) (that are significant at greater than 95% level). Thus, there has been a long-term increase of RWB events on the equator side of the jet, as the jet has moved poleward. This link between RWB frequency and jet location also occurs for year-to-year variations, with a significant correlation between interannual anomalies in jet latitude and RWB frequency (not shown).

The trends in RWB on the poleward side of the jet differ from that on the equatorward side. There is still large year-to-year variability (Figure 1(d)), but there are only very weak decreasing trends in the frequency of RWB around 60°S that are not statistically significant, see Figure 1(d) and (e).

The RWB trends shown here are consistent with those identified with the alternative algorithm used by Wang and Magnusdottir (2011). They found a positive trend in AWB in mid-latitudes (30–60°S) and an insignificant negative trend in CWB in mid- to high latitudes (45–75°S).

4. CAM3 integrations

The relative impact of increasing GHGs and ozone depletion on RWB cannot be determined from the above data analysis alone. However, model integrations can be used to infer the cause of these changes. In this section we repeat the above analysis using the output from the series of CAM3 integrations used by Polvani *et al.* (2011), in which changes in GHGs and stratospheric ozone are independently varied.

We first review the structure of the zonal mean flow in these integrations. The climatological zonal

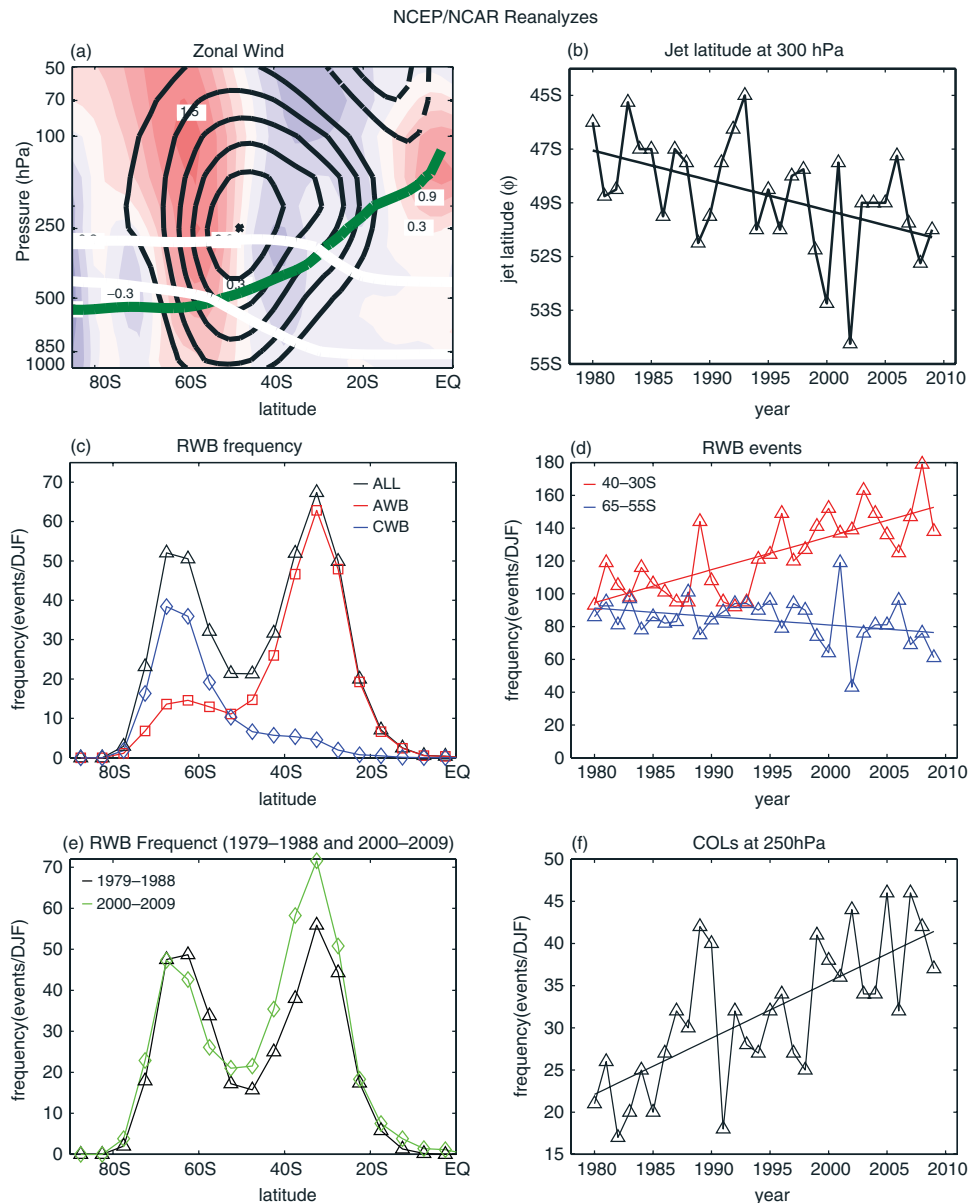


Figure 1. Zonal winds and RWB in the NCEP/NCAR reanalyses. (a) Trends in zonal mean winds from 1979 to 2009 (red/blue shading, with contour intervals of $0.15 \text{ m s}^{-1} \text{ decade}^{-1}$), together with the mean jet (thick black contours), the 310 and 340 K isentropic surfaces, and $PV = -2 \text{ PVU}$ contour (green curve). (b) Time series (curve) and trends (straight line) of the latitude of the maximum wind at 300 hPa. (c) Probability distribution function of RWB frequency per latitude for CWB (blue), AWB (red), and all RWB (black) events. (d) Time series (curve) and trends (straight line) of RWB between 30–40°S (red) and 55–65°S (blue). (e) As in (c) except for all RWB between 1979 and 1988 (black) and between 2000 and 2009 (green). (f) Time series (curve) and trends (straight line) of COLs between 20 and 50°S. Trends shown in panels (b), (d), and (f) are statistically significant except for the decreasing trend in RWB between 55 and 65°S in (d).

mean flow jet in the BOTH2000 integration (which has SSTs, GHGs, and ozone specified at 2000 levels) is shown in Figure 2(a) (black contours), and can be compared with the observed 1979–2009 climatology in Figure 1(a). There is reasonable agreement between the simulated and observed jets, although it is notable that the climatological jet in the model is stronger, higher, and slightly equatorward compared to the reanalyses.

The differences in zonal winds between the REF1960 and BOTH2000 integrations are also shown in Figure 2(a). Comparing with Figure 1(a) we again see qualitative agreement with the observed change

in SH winds, i.e. there is a deceleration of zonal winds equatorward of the jet and acceleration poleward of the jet. There are differences in the tropics, but the focus here is changes surrounding the westerly jet. As shown by Polvani *et al.* (2011), comparison of the four integrations shows that the changes in zonal winds are dominated by ozone depletion in the stratosphere. Specifically, the change in zonal winds between the OZONE2000 and REF1960 is similar to that shown in Figure 2(a), whereas there are only small differences between GHG2000 and REF1960, see figure 4 of Polvani *et al.* (2011). The location of the upper tropospheric jet for the four integrations is

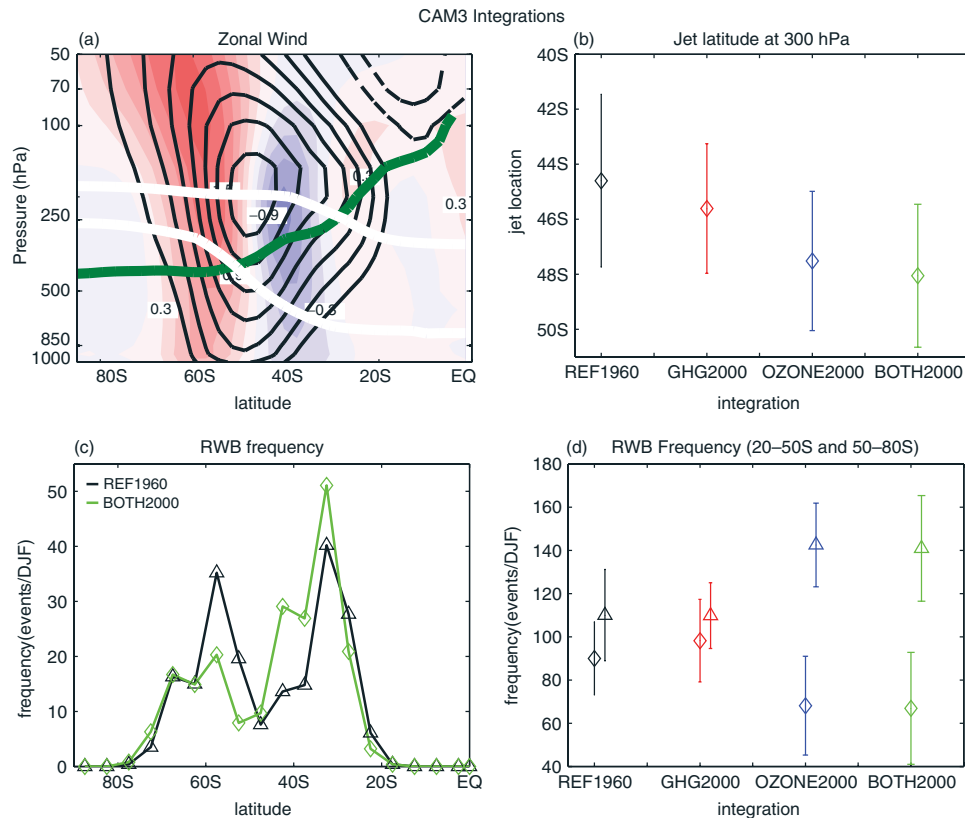


Figure 2. (a) Differences in zonal-mean zonal wind between the BOTH2000 and REF1960 integrations, together with mean jet for BOTH2000. Quantities shown are as in Figure 1(a). (b) Mean latitude of the maximum wind at 300 hPa for each integration. Vertical bars show plus and minus one standard deviation. (c) As in Figure 1(e), except for REF1960 (black) and BOTH2000 (green) integrations. (d) Frequency of RWB between 20–50°S (triangles) and 50–80°S (diamonds) for each integration.

shown in Figure 2(b): the mean jet in OZONE2000 and BOTH2000 is around 3° south of that in REF1960, whereas the jet location in GHG2000 is similar to that in REF1960. (Similar variations are found in the jet location at 850 hPa, see figure 5 of Polvani *et al.* (2011).)

We now examine the occurrence of RWB in the CAM3 integrations. Given the resolution of the model it is not clear how well synoptic-scale RWB events are simulated, so we first evaluate the realism of the RWB in the BOTH2000 integrations. The latitudinal variation of RWB events in BOTH2000 is shown in Figure 2(c), and consistent with the reanalyses (Figure 1(c)), there is a minimum at the jet maximum with local maxima in RWB either side of the jet. Also, again consistent with the reanalyses, there is more RWB on the equatorward side of the jet (although the difference is larger in CAM3), and RWB on the equatorward side is mainly anticyclonic, with cyclonic breaking occurring predominantly on the poleward side (not shown). However, the frequency of RWB is lower in CAM3 than in the reanalyses. Comparisons of composites of RWB from CAM3 with those from NCEP/NCAR reanalyses show that both the PV structure and wave fluxes of RWB events in CAM3 are similar to those observed, although the RWB in CAM3 tends to have a smaller spatial scale (not shown).

We next consider changes in the frequency of RWB events among the integrations. Figure 2(c) shows that

there is an increase in the number of RWB events on the equatorward side of the jet and a slight decrease in RWB events on the poleward side in the BOTH2000 integration relative to the reference REF1960 integration (see also Figure 2(d)). These changes in RWB frequency are qualitatively consistent with the observed trends over the last 30 years. Similar differences are found between the OZONE2000 and REF1960 integrations, but there are only very small differences in RWB between GHG2000 and REF1960 (Figure 2(d)). These changes in RWB are consistent with the changes in zonal winds between integrations, i.e. there is a large change in RWB frequency between integrations where there is a large change in the jet location. Furthermore, these results support the hypothesis that it is stratospheric ozone depletion, and not increases in GHGs, that has caused the observed changes in RWB in the SH. The frequency of RWB in the CAM3 integrations has also been examined in other seasons, but the changes between integrations were not significant. This is consistent with the lack of significant changes in the jet location among the CAM3 integrations for other seasons (Polvani *et al.*, 2011).

5. Conclusions

Examination of NCEP/NCAR reanalyses for the last 30 years shows that during austral summer there have

been simultaneous changes in the location of the eddy-driven jet and the number of RWB events on the tropopause, with an increase in the number of RWB events on the equatorward side of the jet and weak decrease on the poleward side of the jet (see also Wang and Magnusdottir, 2011). These changes are captured within time-slice CAM3 integrations in which forcing fields are from 1960 to 2000 conditions. Furthermore, the large change in RWB frequency occurs if only stratospheric ozone is changed. There are only small changes in RWB frequency when GHGs and SSTs alone are changed. This indicates that stratospheric ozone depletion is likely the dominant cause of the changes in the RWB.

The exact mechanisms by which ozone depletion, and the resulting strengthening of the Antarctic polar vortex, influences the tropospheric flow are not fully understood. Several different mechanisms have been proposed, including the balanced response to stratospheric PV anomalies, and the impact of the lower stratospheric winds on the phase speed, meridional propagation, and wave breaking of tropospheric synoptic eddies (e.g. Gerber *et al.*, 2012, and references therein), but there is no consensus on which is the primary mechanism. There is also uncertainty in the causal relationship between the tropospheric jet location and RWB frequency, with indications that there is a positive feedback between the position of the jet and RWB (e.g. Rivière, 2009).

RWB events have been linked to different other types of weather systems, and the above RWB trends may result in trends in these systems. One example of weather systems connected to RWB is COLs. Ndarana and Waugh (2010) showed that in the SH nearly all COLs occur downstream and after or during RWB events or intrusions of high PV. Analysis of the 250 hPa COLs, as identified in Ndarana and Waugh (2010), shows a large, statistically significant, and positive trend in mid-latitude COLs during DJF (Figure 1(f)). The COL trend closely follows the mid-latitude RWB trend (i.e. similar relative increase in frequency over the 30 years), suggesting that the trends in RWB may alter the occurrence of severe weather systems that are connected with COLs. Further analysis is needed to examine if the RWB trends are linked to trends in other weather systems, e.g. blocking highs or precipitation events (e.g. Kang *et al.*, 2011). It would also be of interest to examine regional aspects of the trends, in RWB as well as related weather systems.

Acknowledgements

This work was funded by the US National Science Foundation and the South African National Research Foundation.

References

Collins WD, Bitz CM, Blackmon ML, Bonan GB, Bretherton CS, Carton JA, Chang P, Doney SC, Hack JJ, Henderson TB, Kiehl JT,

- Large WG, McKenna DS, Santer BD, Smith RD. 2006. The Community Climate System Model Version 3 (CCSM3). *Journal of Climate* **19**: 2122–2143.
- Cionni I, Eyring V, Lamarque JF, Randel WJ, Stevenson DS, Wu F, Bodeker GE, Shepherd TG, Shindell DT, Waugh DW. 2011. Ozone database in support of CMIP5 simulations: results and corresponding radiative forcing. *Atmospheric Chemistry and Physics* **11**: 10875–10933.
- Gerber E, *et al.* 2012. Assessing and understanding the impact of stratospheric dynamics and variability on the earth system. *Bulletin of the American Meteorological Society*. (in press).
- Hu Y, Fu Q. 2007. Observed poleward expansion of the Hadley circulation since 1979. *Atmospheric Chemistry and Physics* **7**: 5229–5236.
- Kalnay E, Kamitsu M, Kistler R, Collins W, Deaven D, Gandil L, Iredell M, Saha S, White G, Woolen J, Zhu Y, Cheliah M, Ebisukazi W, Higgins W, Janowiak J, Mo KC, Ropelewski C, Wang W, Leetmaa A, Reynolds R, Jenne R, Joseph D. 1996. The NCEP/NCAR 40 Year Reanalysis Project. *Bulletin of the American Meteorological Society* **77**: 437–471.
- Kang S, Polvani LM, Fyfe JC, Sigmond M. 2011. Impact of polar ozone depletion on subtropical precipitation. *Science* **332**: 951–954.
- McIntyre ME, Palmer TN. 1983. Breaking planetary waves in the stratosphere. *Nature* **305**: 593–600.
- McLandress C, Shepherd T, Scinocca J, Plummer D, Sigmond M, Jonsson A, Reader C. 2011. Separating the dynamical effects of climate change and ozone depletion: Part 2. Southern hemisphere troposphere. *Journal of Climate* **24**: 1850–1868.
- Nakicenovic N, Swart R. 2000. Special Report on Emissions Scenarios: A special report of Working Group III of the Intergovernmental Panel on Climate Change. Cambridge University Press: Cambridge, UK; 599 pp.
- Ndarana T, Waugh DW. 2010. The link between cut-off lows and Rossby wave breaking in the Southern Hemisphere. *Quarterly Journal of the Royal Meteorological Society* **136**: 869–885.
- Ndarana T, Waugh DW. 2011. A climatology of Rossby wave breaking on the Southern Hemisphere tropopause. *Journal of the Atmospheric Sciences* **68**: 798–811.
- Pelly JL, Hoskins BJ. 2003. A new perspective on blocking. *Journal of the Atmospheric Sciences* **60**: 743–755.
- Polvani LM, Waugh DW, Correa GJP, Son S-W. 2011. Stratospheric ozone depletion: the main driver of 20th century atmospheric circulation changes in the Southern Hemisphere. *Journal of Climate* **24**: 795–812.
- Previdi M, Liepert BG. 2007. Annular modes and Hadley cell expansion under global warming. *Geophysical Research Letters* **34**: L22701. DOI: 10.1029/2007GL031243.
- Rayner NA, Parker DE, Horton EB, Folland CK, Alexander LV, Rowell DP, Kent EC, Kaplan A. 2003. Global analyses of sea surface temperature, sea ice, and night marine air temperature since the late nineteenth century. *Journal of Geophysical Research* **108**: 4407. DOI: 10.1029/2002JD002670.
- Rivière G. 2009. Effect of latitudinal variations in low-level baroclinicity on eddy life cycles and upper-tropospheric wave-breaking processes. *Journal of the Atmospheric Sciences* **66**: 1569–1592.
- Son S-W, Tandon NF, Polvani LM, Waugh DW. 2009. Ozone hole and southern hemisphere climate change. *Geophysical Research Letters* **36**: L15705. DOI: 10.1029/2009GL038671.
- Sprenger M, Wernli H, Bourqui M. 2007. Stratospheric-troposphere exchange and its relation to potential vorticity streamers and cutoffs near the extratropical tropopause. *Journal of the Atmospheric Sciences* **64**: 1587–1602.
- Thompson DWJ, Solomon S. 2002. Interpretation of recent Southern Hemisphere climate change. *Science* **296**: 895–899.
- Wang Y-H, Magnusdottir G. 2011. Tropospheric Rossby wave breaking and the SAM. *Journal of Climate* **24**: 2134–2146.